UNIVERSITY OF WISCONSIN LA CROSSE

Graduate Studies

CHARACTERIZATION OF HPIV3 MATRIX MUTANTS DEFICIENT IN BUDDING

A Manuscript Style Thesis Submitted in Partial Fulfillment of the Requirements for the Degree of Master of Science

Jacob Schmidt

College of Health and Science

Microbiology

December, 2019

CHARACTERIZATION OF HPIV3 MATRIX MUTANTS DEFICIENT IN BUDDING

By Jacob Schmidt

We recommend acceptance of this thesis in partial fulfillment of the candidate's requirements for the degree of Master of Science in Microbiology

The candidate has completed the oral defense of the thesis.

Michael Hoffman, Ph.D. — 12-2-19 — Date
Thesis Committee Chairperson

Scott Cooper, Ph.D. — 12-2-19 — Date
Thesis Committee Member

Peter Wilker, Ph.D. — 12-2-19 — Date
Thesis Committee Member

Anton Sanderfoot, Ph.D. — 12-2-19 — Date
Thesis Committee Member

Thesis accepted

Meredith Thomsen, Ph.D. — 12-9-19 — Date
Graduate Studies Director

ABSTRACT

Schmidt, J.L. Characterization of HPIV3 matrix mutants deficient in budding. MS in Microbiology, December 2019, 50 pp. (M. Hoffman)

The matrix (M) protein of human parainfluenza virus type 3 (HPIV3) is important for directing assembly and release of new virus; however, the mechanism of release remains unclear. Identifying domains of M required for proper function can help to better understand HPIV3. Alanine amino acid substitutions in regions of M result in inhibition of growth of HPIV3 and release of M protein from cells. Phenotypic revertants, containing a second site amino acid change in M, of the original amino acid substitutions have been isolated and restore growth of HPIV3. Through generation of a 3-D homology model it was hypothesized and confirmed the original alanine substitution regions are important for dimerization of M. The regions were also shown to be unessential for nuclear localization through immunofluorescent microscopy. M proteins containing the second site amino acid change did not restore dimerization of M, but could may restore oligomerization or some other function of M.

ACKNOWLEDGEMENTS

First, I would like to thank my thesis advisor, Michael Hoffman, PhD, who provided knowledge and guidance throughout my graduate studies. I also want to thank my thesis committee members Scott Cooper, PhD, Anton Sanderfoot, PhD, and Peter Wilker, PhD, for providing feedback, guidance, and suggestions. Additionally, I would like to thank the University of Wisconsin La Crosse Research, Service, Education, and Leadership (RSEL) grant for helping to fund my graduate research.

TABLE OF CONTENTS

PAGE

LIST OF FIGURES vii

INTRODUCTION 1

Clinical Significance 1

HPIV3 Taxonomy and General Characteristics 2

Virion Structural Organization 3

General Life Cycle of HPIV3 5

Adsorption and Entry 5

Transcription and Replication 5

Assembly and Release 6

Matrix Protein Activities and Functions 6

Self-association 7

Nucleocapsid Interactions 8

Membrane Interactions 8

Glycoprotein Interactions 9

Host-cell Protein Interactions 9

Nuclear Trafficking of Matrix 11

HPIV3 Matrix Proteins 12

Importance of 54-YLDV and 300-YPLMDL Domains 13

Research Objectives 19

MATERIALS AND METHODS 21

Creation of a 3-D Homology Model 21

Cell Culture 21

Plasmids 21

Immunofluorescent Microscopy 22

CheckMate™ Mammalian Two-Hybrid System 23

RESULTS 24

Generation of a 3-D Homology Model of HPIV3-M 24

Assessment of M Self-Association Disruption and Restoration 27

Assessment if localization is affected by perturbations of M 29

DISCUSSION 32

REFERENCES 36

LIST OF FIGURES

FIGURE PAGE

1. Human parainfluenza virus 3 virion 4
2. Model of ESCRT pathway utilization by viral matrix protein 10
3. Release of alanine substitution M proteins 300-305 16
4. Release of alanine substitution M protein 54-57 16
5. HPIV3 growth curve of alanine substitution mutants 17
6. HPIV3 growth curve of phenotypic revertants 19
7. HPIV3 Matrix protein model (1) 25
8. HPIV3 Matrix protein model (2) 26
9. Sections of Human parainfluenza virus type 3 Matrix protein model 27
10. Localization of 300-305 region mutants and revertants 31

INTRODUCTION

Clinical Significance

Human parainfluenza viruses (HPIV) are a frequent cause of community acquired acute respiratory infections worldwide (1). Acute respiratory infections encompass both upper and lower respiratory tract infections. The upper respiratory tract extends through the airways of the nostrils to the voice box of the larynx (2). The lower respiratory tract includes airways from the trachea to the alveoli of the lungs (2). Acute respiratory infections are the leading cause of morbidity and mortality among children under five years of age and cause an estimated 156 million episodes of clinical pneumonia alone worldwide (2,3). Of these clinical pneumonia cases, 8.7% were severe enough to require hospitalization (3). Although most lower respiratory infections are thought to be bacterial in nature, there are estimates of 40 to 50 percent of infections in infants and children being caused by viral agents in developing countries (3). Additionally, a recent comprehensive study of causes of severe pneumonia in children has found 60% of cases being caused by viral agents (4). The leading causes of viral pneumonia are human respiratory syncytial virus (HRSV), followed by HPIV. HPIVs are genetically and antigenically broken into types 1-4 (1). In children < 5 years, HPIV types 1-3 have been found in as many as a third of the 5 million lower respiratory infections per year in the U.S. (1). Additionally, HPIV types 1-3 were responsible for 12% of hospitalizations for lower respiratory infections in the U.S. in persons younger than 18 years (1). Previous infection does not confer lifelong immunity to HPIV and reinfection into adulthood

occurs (1,5,6). However, the first HPIV infections, especially HPIV3, seem to pose the most threat to infants and children as they are usually the most severe. With HPIV3 40% of infections occur in the first year of life (1). It is estimated that HPIV3 is responsible for approximately 18,000 hospitalizations in infants and children every year in the U.S. (1). There is currently no vaccine or drugs available for treatment.

HPIV3 Taxonomy and General Characteristics

HPIV3 is classified within the order of *Mononegavirales*. Members of *Mononegavirales* have enveloped virions, helically symmetrical nucleocapsids, and non-segmented, single stranded, (-) sense RNA genomes (6,7). The *Mononegavirales* is comprised of five families: *Bornaviridae*, *Filoviridae*, *Rhabdoviridae*, *Pneumoviridae*, and *Paramyxoviridae*. *Filoviridae*, *Rhabdoviridae*, and *Paramyxoviridae* can typically be distinguished from one another through morphology of virions (7,8). *Filoviridae* virions are identifiable by their bacilliform shape (7). The most notable filovirus is Ebola virus, due to the severe hemorrhagic fever it causes in humans (8). *Rhabdoviridae* members are easily distinguishable by their bullet-shaped virions (7). The most notable viruses within *Rhabdoviridae* are Rabies virus, and vesicular stomatitis virus (VSV). Rabies virus infects humans and other mammals, and causes acute progressive encephalitis in humans (7). Vesicular stomatitis virus primarily infects non-human mammals, and affects domesticated animals (cattle, horses, pigs) causing fever and lesions (12).

The *Paramyxoviridae* and *Pneumoviridae* families have virions with morphologies ranging from filamentous to pleomorphic to spherical with varying diameters (7,8). HRSV is within the *Pneumoviridae* family ~~which~~that, as mentioned earlier, is the leading cause of viral pneumonia in children <5 years (3,7).

Paramyxoviridae contains the following genera: *Rubulavirus*, *Avulavirus*, *Respirovirus*, *Henipavirus*, and *Morbillivirus* (7). The type species of the genera are, respectively: mumps virus (MuV), Newcastle disease virus (NDV), Sendai virus (SeV), Hendra virus (HeV), and measles virus (MeV) (6). The four types of HPIV are spread between the genera *Rubulavirus* (HPIV-2 and HPIV-4) and *Respirovirus* (HPIV-1 and HPIV-3) (1,7).

Virion Structural Organization

HPIV3 virions are 150-250 nm in diameter and range in morphology from spherical to pleomorphic to filamentous (1). Virions consist of the following six structural proteins: hemagglutinin-neuraminidase (HN), fusion (F), nucleoprotein (N), phosphoprotein (P), large protein (L), and matrix (M) (Fig. 1). The genome also encodes a seventh protein, nonstructural C protein, in an alternate reading frame in the P gene (8,13). The function of C is not fully understood. It may be involved in the regulation of viral transcription, inhibiting the host cell immune response and the promotion of virus particle release (14,15).

The exterior of the virion consists of an envelope and two embedded glycoproteins (HN and F) (8,13). The envelope is acquired from the plasma membrane when virions bud out of cells. The HN protein is 572 amino acids long with the majority of the protein (aa 53-572) being on the exterior of the envelope (49). The remainder of the protein consists of a transmembrane domain (aa 31-52) and an amino-terminal cytoplasmic tail (aa 1-31) (49). The HN protein is in a tetrameric form when present on virions (49). The protein has both sialic acid binding activity, allowing for hemagglutination, and neuraminidase activity (sialic acid cleavage, 7,12). Both activities are contained in the exovirion domain of the protein (7). The F protein also contains

exovirion (aa 19-493), transmembrane (aa 494-514), and carboxy-terminal endovirion domains (aa 515-539) (48). The F protein exists as a trimer on virions and, after attachment, mediates fusion of the viral envelope with host cell membranes (7,15).

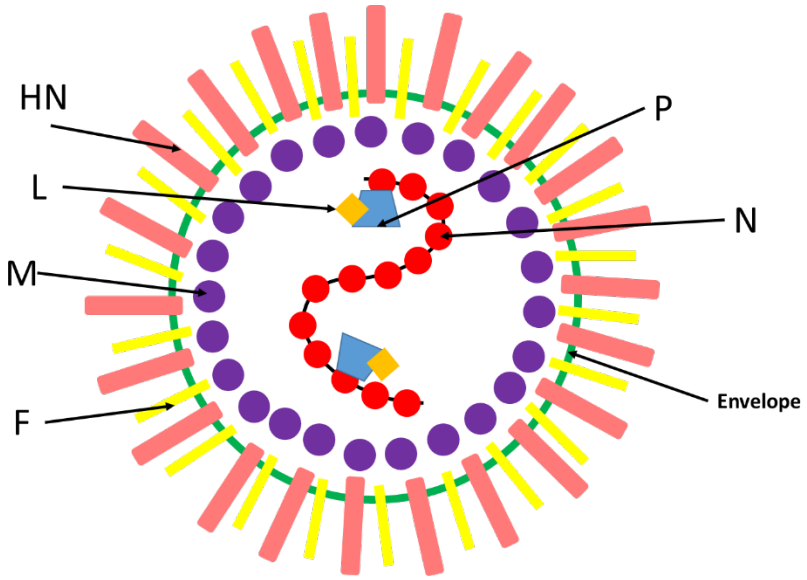

Figure 1. Human parainfluenza 3 virion

The interior of virions contain the nucleocapsid core of the virus, termed the N-RNA, consisting of the single-stranded, (-) sense RNA genome helically encapsidated by N (7). The order of genes encoded on the genome from 3' to 5' is N, P/C, M, F, HN, and L. The L and P proteins are also closely associated with the N-RNA via interactions with N, to form a ribonucleoprotein complex (RNP) (7,12). The L and P proteins form the RNA-dependent, RNA polymerase required to transcribe the genome upon entry into a cell (5,7). The L-P complex also carries out replication of the viral genome.

The most abundant protein in HPIV3 virions is M, which lines the inner layer of the envelope where it likely interacts with the envelope directly as well as the cytoplasmic tails of HN and F, and N (7,12,16). M plays a critical role in the viral life cycle by facilitating assembly and budding of new virions (5,7).

General Life Cycle of HPIV3

Adsorption and Entry

Infection of a cell by HPIV3 virions begins through attachment of HN to cell surface proteins containing sialic acid (sialoglyconjugates) (5,7). HN and F then regulate the fusion process of the viral envelope with host cell membrane (5). The fusion of envelope and host cell membrane allows for the virion to empty the RNP into the host cell.

Transcription and Replication

Upon entry of the genome into host cells, transcription is the next event to occur (5,7). The P-L complex functions as an RNA-dependent, RNA polymerase. It begins transcription of the viral RNA starting at the 3' end of the genome (7). Transcription of the genome is done via a start-stop mechanism, initiating and terminating transcription at the beginning and end of each individual gene (5). This results in the production of six individual capped and polyadenylated mRNAs encoding the proteins N, P, M, F, HN, and L (5,7). Transcribed RNAs can then be translated into viral proteins by host ribosomes. Following initial transcription and accumulation of viral proteins, replication of the genome begins (7). Replication begins with the entire (-) sense genome being copied into a single genome-length (+) sense RNA known as the antigenome (5). The antigenomes can then serve as templates for replication of new HPIV3 (-) sense genomes (5,7). The

newly made genomes are immediately encapsidated by N, and can be transcribed into more mRNAs, replicated, or packaged into new HPIV3 virions.

Assembly and Release

Assembly of virus particles occurs on the inner surface of the plasma membrane. Envelope glycoproteins (HN and F) are directed to the cellular plasma membranes after translation in the rough endoplasmic reticulum via the secretory pathway (5,17). M localizes to the plasma membrane post-translation, though it may transit through the nucleus first (5,17,22). Initiation of nucleocapsid assembly begins with the binding of N to viral RNA as it is synthesized (7,12). Formation of the N-RNA allows for interactions with L, P, and M (12,17). To facilitate assembly, matrix proteins are able to interact with the nucleocapsid (N protein in particular) and envelope proteins. Once assembly is complete, mature virions bud from cells. The budding mechanism is currently being studied, though matrix proteins seem to be pivotal to this process as well. The neuraminidase activity of HN cleaves sialic acids present on the infected cell to prevent reinfection of the cell via the hemagglutinin activity of HN, upon budding of virions (7).

Matrix Protein Activities and Functions

The matrix proteins of paramyxoviruses have been extensively studied due to their role in the assembly and budding of new virions. The importance of M in the assembly and release of viral particles was first proposed through analysis of mutant measles and Sendai viruses that were deficient in producing viral particles (50-52). M protein was inactivated or undetectable in the various budding deficient mutants, leading to the conclusion that M was crucial in formation of virions (50-52). Providing further evidence that the M protein is involved in budding is the observation that expression of

M alone, without any other viral proteins, is sufficient for producing virus-like particles (VLPs) which are released vesicles consisting of M protein surrounded by an envelope. This independent budding feature of M is observed in HPIV1, HPIV3, SeV, NDV, Nipah virus (NiV), and MeV (22,26,38,49,53-58). PIV5 and MuV proteins are also able to produce VLP's, but require co-expression of M, N and either the F or the HN proteins (27,28).

In order to mediate assembly and release, the M protein is capable of a multitude of interactions and functions. Matrix proteins have been shown to be able to self-associate, interact with membranes, viral glycoproteins, nucleocapsids, and host cell proteins (13,18,19). An additional, recently recognized activity of M proteins is their ability to transit through the nucleus (23,42-44,59-62). This nuclear localization seems to be important for M's function in viral budding. The activities of M proteins are further discussed in the following sections.

Self-association

Matrix proteins have been shown to self-associate into dimers, and higher-order oligomers as well (6). This self-association of M proteins has been shown through co-immunoprecipitations, cross-linking, electron microscopy, and X-ray crystallography. (20,24,69-71). For example, M proteins of canine distemper virus and HPIV3 have both been shown to interact with themselves via co-immunoprecipitations (41,74). Freeze-fracture analyses of cells infected with SeV, also show lattices of M arranged on membranes (13). Crystal structures of M proteins of the paramyxovirus NDV and the pneumovirus RSV also indicate they occur in dimers, and contain contacts allowing for

dimer-dimer interactions (20, 24). It has been theorized that formation of M lattices could even cause membrane deformations and begin the process of virion budding (20,24).

Nucleocapsid Interactions

Matrix proteins of paramyxoviruses are also capable of interacting with the RNP complexes formed in infected cells. RNPs of MeV will colocalize with M at the plasma membrane of an infected cell (19). However, this colocalization is lost when M is mutated in MeV (19). This interaction is mediated by a direct interaction between the nucelocapsid protein and M (19). Yeast two-hybrid assays using measles proteins have mapped these interactions to the C-terminal portion of nucleocapsid protein (68).

Membrane Interactions

Matrix proteins contribute to assembly through interactions with the plasma membrane of cells, which will eventually form the viral envelope. Matrix proteins have been shown to interact with membranes through electron microscopy as well as fractionation studies (13). The lack of any domains capable of spanning a membrane indicate that this interaction is peripheral (6,13). There is evidence of both electrostatic and hydrophobic interactions being drivers of membrane association. Matrix proteins of paramyxoviruses are rich in basic amino acids having a net charge at pH 7 between +14-17, and isoelectric points typically between 9.0-9.6 (8,49,63-65). The highly positive charge on M proteins would indicate a possible electrostatic interaction with the polar heads of the phospholipids of the cell membrane. Mapping of highly positive surface domains on crystallized structures of NDV and HRSV M proteins support this idea (20, 77). However, there is also evidence M will associate with liposomes regardless of the net charge of the lipid membranes (13). This would indicate hydrophobic interactions

between the two may also contribute to the association in addition to the electrostatic interactions.

Glycoprotein Interactions

There is also evidence of interactions between the cytoplasmic tails of viral glycoproteins and M. The clearest evidence of this interaction can be seen by the loss of M-glycoprotein co-localization when cytoplasmic tails of various paramyxoviruses are truncated (19,21). Interactions between the two can also be show by co-immunoprecipitation. In NDV direct HN-M interactions were shown via co-immunoprecipitation (22). The M proteins of Sendai virus also form detergent resistant membrane rafts upon co-expression of M and viral glycoproteins (66).

Host-cell Protein Interactions

Paramyxoviruses' M proteins not only interact with other viral proteins, but interact with host cell proteins as well. It has been shown Sev M proteins interact with the endosomal sorting complexes required for transport (ESCRT) system (18,19). Proteins which make up the ESCRT system are normally responsible for cytokinesis as well as forming multivesicular bodies (MVBs) (39). Formation of MVBs starts with ESCRT complexes recognizing ubiquitinated protein on an endosomal membrane. The targeted protein ends up in a vesicle within the endosome (which would be an MVB) where it is degraded. The ESCRT machinery mediates this process by causing membrane invagination into the endosome then triggering membrane fission, away from the cytoplasm, allowing the vesicle to bud into the endosome (Fig. 2.) (39).

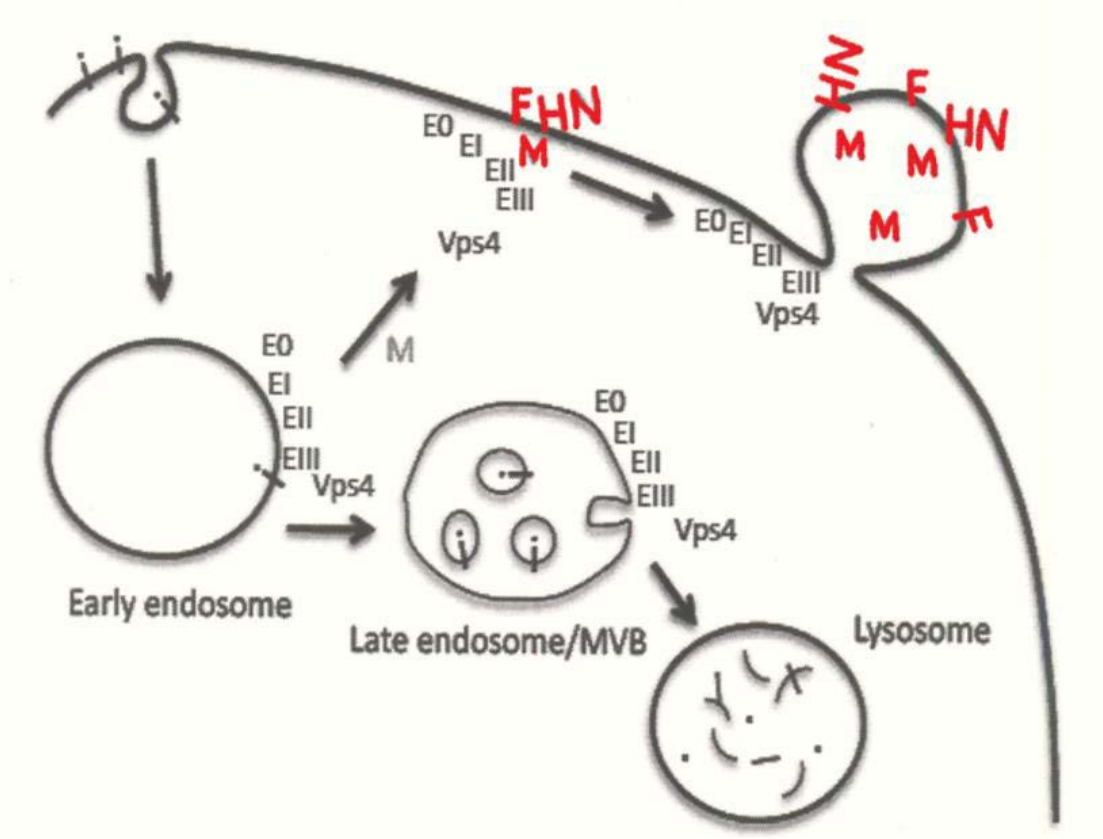

Figure 2. Model of ESCRT pathway utilization by viral matrix protein (viral proteins in red). The ESCRT complexes are sequestered away from the endosome to the plasma membrane via interactions with the M protein. Once at the budding site, ESCRTs then facilitate budding. Figure produced by Christine Hulseberg (76).

Some viruses are able to highjack this machinery and cause this same process to occur at the plasma membrane for formation of enveloped virions (18,19). They can accomplish this by having viral proteins directly interact with the ESCRT machinery. Conserved amino acid sequences interacting with the ESCRT machinery have been identified and given the term late domains (40). These late domains were first characterized in retroviral Gag proteins and include: P(T/S)AP, PPxY, and $YP(X)_nL$ (where n = 1 or 3 aa, 18). These late domain sequences are also found in (-)-RNA viruses

as well, including rabies virus, VSV, Ebola virus, LCMV, and Lassa fever virus (19,29-36). The paramyxovirus, SeV, has also been shown to interact with ESCRT machinery (the ALIX/Aip1 protein) via a YLDL sequence (believed to be a version of the $YP(X)_nL$ late domain) in its M protein (25). PIV5 and MuV M proteins also likely use ESCRT for budding since they become deficient in producing VLPs, when co-expressed with a dominant-negative Vps4 mutant protein, a critical ESCRT protein involved in recycling of ESCRT components (27,28). However, some paramyxoviruses (HRSV and NiV) are able to still produce VLPs efficiently when expressed using the same Vps4 mutated proteins, and so may bud through a different mechanism (37,38).

Paramyxovirus M proteins have also been shown to interact with host proteins other than ESCRT system proteins. For example, SV5 interacts with an integral membrane protein Caveolin 1 (72). Caveolin 1 is clustered at areas of SV5 budding, co-localizes with M in cells, and can be co-immunprecipitated with M. Additionally, it is incorporated into mature virions. MeV has also been shown to interact with a membrane-directed host protein, Annexin A2 (73). Knockdown of Annexin A2 inhibited viral growth and localization of M protein to the plasma membrane.

Nuclear Trafficking of Matrix

Although transcription and replication of paramyxoviruses occurs in the cytoplasm, there is evidence of paramyxovirus M proteins trafficking through the nucleus. This nuclear trafficking of M is an important prerequisite for budding in NiV (44). Disrupting either nuclear localization or nuclear export both decreased NiV VLP formation (44). The following members of *Paramyxoviridae* also demonstrated nuclear trafficking of their matrix protein: HeV, SeV, MuV, MeV, HRSV, and NDV (23,42-44).

The function of this transit is not fully understood. There are several potential advantages to nuclear trafficking including down regulating antiviral host cell responses and/or affecting gene transcription of the host cell to promote replication of the virus. Another observation is that some M protein trafficking through the nucleus becomes ubiquitinated within a nuclear localization signal (NLS). This would disrupt recognition of the NLS and lead to more cytoplasmic localization of the protein. It is also possible that ubiquitination of the M protein is needed for M protein function in budding. NiV, HeV, SeV, MuV, NDV, PIV5, and MeV matrix proteins are ubiquitinated (23,45). Depletion of free ubiquitin in a cell using MG132 treatment caused the matrix protein of these viruses to be retained in the nucleus and inhibited the ability of these viruses to effectively bud (23,44). The mechanism of how ubiquitination of M proteins contributes to viral budding is not understood.

HPIV3 Matrix Proteins

The M protein of HPIV3, as with other paramyxoviruses, is a critical component for viral assembly and budding. M protein expression in tissue culture cells triggers the release of M-containing VLPs. This was demonstrated by transfection of pCAGGS plasmids encoding the HPIV3 M gene into 293T cells and detection of M protein in the media by centrifugation/sedimentation of VLPs through 20% sucrose (26). It was confirmed that released M was in the form of a VLP by the lack of degradation by trypsin or Triton X-100, unless used in combination. The lack of degradation by trypsin alone showed the likelihood of protection of M by an envelope. This shows M protein was not released by cell lysis or other cell-mediated ways but was produced in the form of a VLP. Additionally, M would not be present after centrifugation through the sucrose cushion if

it were released by cell lysis. Expression of viral proteins HN, F, N, and P did not result in VLP formation, indicating M is the only HPIV3 protein with intrinsic budding ability.

HN, F, N, and P were also co-expressed, pair-wise, with M (26). This co-expression resulted in VLPs containing both M and the co-expressed protein (HN, F, or N) indicating the M protein interacts individually with HN, F, and N. Co-expression with P resulted in VLPs containing only M, indicating no direct interaction between M and P. Expressing P in combination with M+N resulted in the presence of P in VLPs, likely due to interactions between N and P. These results showed M drives assembly through interactions with HN, F, and N.

Importance of 54-YLDV and 300-YPLMDL Domains

The 352 amino acid sequence of M was analyzed for the presence of potential late domain sequences, to shed more light on the mechanism behind HPIV3 release. Four potential late domain motifs were identified: 47-PPKH, 54-YLDV, 300-YPLMDL, 338-YPNI (where the number reflects the amino acid position and the letters are the standard one-letter code for amino acids). The presence of functional late domains could mean HPIV3 M facilitates budding using ESCRT machinery. Mutational analysis of the four potential domains, showed alanine substitutions of the 54-YLDV and 300-YPLMDL amino acids reduced VLP formation. Another lab also assessed the budding ability of HPIV3 M mutated in these motifs and found similar results for alanine substitution at residues 302 and 305, but they did not report deficiencies of VLP production for a deletion of the 54-YLDV motif (41). The conflicting results could be due Hoffman's lab using wild-type M, whereas Zhang et. al used an HA-tagged M protein for visualization. Reduced budding of tagged M proteins may reduce the sensitivity of VLP assays (26,41).

Although these amino acid patterns were similar to characterized late domain amino acid patterns, the Hoffman lab has not shown M protein interactions with ESCRT proteins. Co-immunoprecipitation assays between HPIV3 M and the ESCRT protein Alix/AIP1 showed no interaction between the two. The lack of an interaction between HPIV3 M and Alix/AIP1 was further confirmed using a mammalian two-hybrid system (Hoffman lab unpublished). Additionally, HPIV3 M-VLP release in siRNA-mediated Alix knockdown within cells showed no inhibition of M release (78). In contrast, work with the closely related SeV has shown that the SeV M binds Alix and that binding is dependent on an YLDL M amino acid motif that aligns with the HPIV3 54-YLDV sequence (25). However, another group showed that suppression of Alix did not affect production of Sendai virions upon a natural infection (79). As a result of this conflicting evidence there isn't a definitive answer for whether or not SeV utilizes Alix as a mechanism for budding. Another critical protein for ESCRT-mediated budding is Vps4, since it plays an essential role in releasing ESCRT complexes from membranes for reuse. However, Vps4 depleted cells showed no inhibition on HPIV3 M release as well (Hoffman lab unpublished).

Since ubiquitination has been linked to paramyxovirus budding and is a sorting signal of the ESCRT system, an analysis of aa 302 as a signal for ubquitination was done. Both the Zhang et. al. lab and the Hoffman lab has performed the same alanine substitution at amino acid position 302 of HPIV3 M and reported similar deficiencies in production of VLP's (41). However, in analysis of ubiquitination of M containing the L302A substitution they had conflicting results. Zhang et. al. concluded HPIV3 M ubiquitination was lost due to the substitution and this caused the VLP deficiency,

whereas the Hoffman lab did not show any difference in ubiquitination following the L302A amino acid substitution of M when compared to wild type M protein (41, Hoffman lab unpublished).

To further characterize the 54-YLDV and 300-YPLMDL regions, additional alanine substitution were generated via mutagenesis of the pCAGGS-M encoding sequence. Since the Y, P, and L residues of the standard $YP(X)_{1,3}L$ late domain (where X indicates any amino acid, and the subscript indicates a range from 1 to 3 amino acids are tolerated in the sequence) are characteristically crucial, the alanine substitutions at positions 54, 55, 57, 300, 301 and 305 would be expected to be most detrimental to HPIV3 budding, if these regions were late domains. In agreement with this prediction VLP formation assays performed with the 300-YPLMDL alanine substitutions showed Y300 and P301 both resulted in a severe disruption in the ability of M to form VLPs (Fig. 3). However, in contradiction to the expected result, substitution at position L305 had only a small negative effect on the ability of M to form VLP's and substitution at L302 had a large negative effect (Fig. 3). Virus like particle assays performed with the 54-YLDV alanine substitutions yielded similar inconsistent results with the expectation of substitution of a YP(X)1,3L late domain. Alanine substitution of 54Y had the least negative effect on VLP formation, whereas alanine substitution of 55L, 56D and 57V had a more significant negative impact (Fig. 4). Notably, expression of the 55L, 56D and 57V alanine substitution M proteins was low, possibly indicating that the mutation triggered misfolding and/or instability of the protein (Fig. 4).

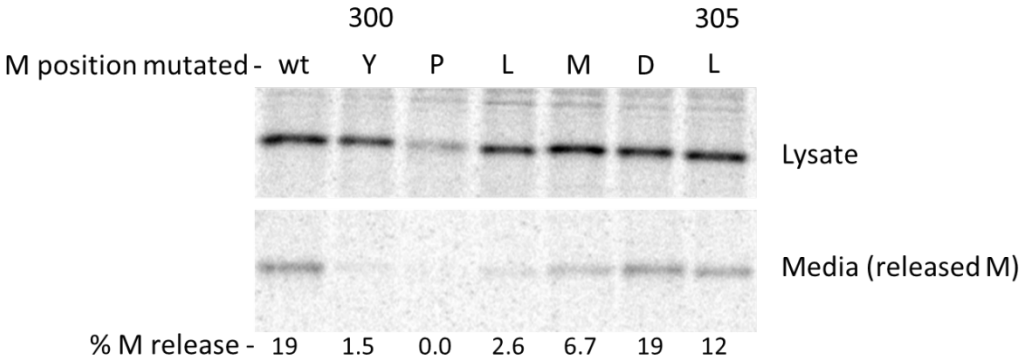

Figure 3. Release of alanine substitution M protein mutants in the form of VLPs. 293T cells were tranfected with pCAGGs encoding wild type HPIV3 M or HPIV3 M with an alanine substitution made at amino acid positions 300, 302, 303, 304, or 305. Matrix protein in the cell lysates and media are compared by a % of total M released into the media.

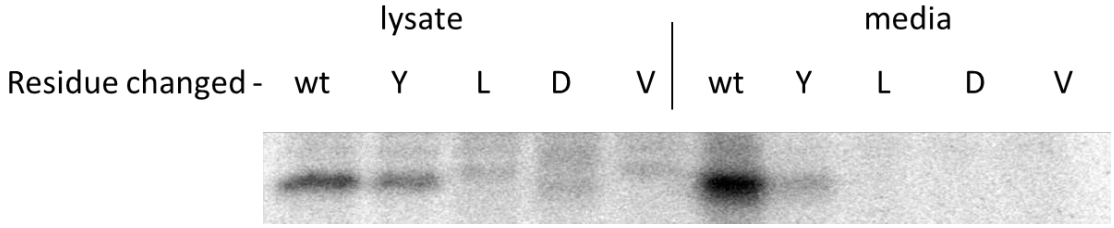

Figure 4. Release of alanine substitution M protein mutants in the form of VLPs. 293T cells were tranfected with pCAGGs encoding wild type HPIV3 M or HPIV3 M with an alanine substitution made at amino acid positions 54, 55, 56, or 57.

Although the function of the regions 54-YLDV and 300-YPLMDL do not seem to be ESCRT pathway-related, they still are important for VLP formation. Therefore, a further analysis of how these regions contribute to M protein function was warranted. Toward this goal, mutant viruses containing single alanine substitutions in the two regions were created. Specifically, viruses containing single alanine substitutions in the HPIV3 M protein at amino acid positions 54, 55, 300, 302, and 305 were created and analyzed.

Perturbations in these regions resulted in defects of the growth of the mutants compared to wild-type HPIV3 (Fig. 5). In the 300-YPLMDL region, the Y300A and L302A mutants (where the first letter indicates the wildtype amino acid and number, and the second letter indicates what that residue was changed to by mutation) severely reduced viral growth, while the L305A mutant had a minor reduction in growth (Fig. 5). In the 54-YLDV region, the L55A mutant also severely reduced viral growth, whereas the Y54A mutant had a minor reduction in growth (Fig. 5). These results of amino acid positions important for viral growth mirror those found for VLP formation. Therefore, the inhibition of virion release correlates with the release of M in a VLP assay. Consequently, since other viral proteins are not present in the VLP assays performed, the deficiencies of these mutants are not likely caused by interactions between M and N, HN, or F.

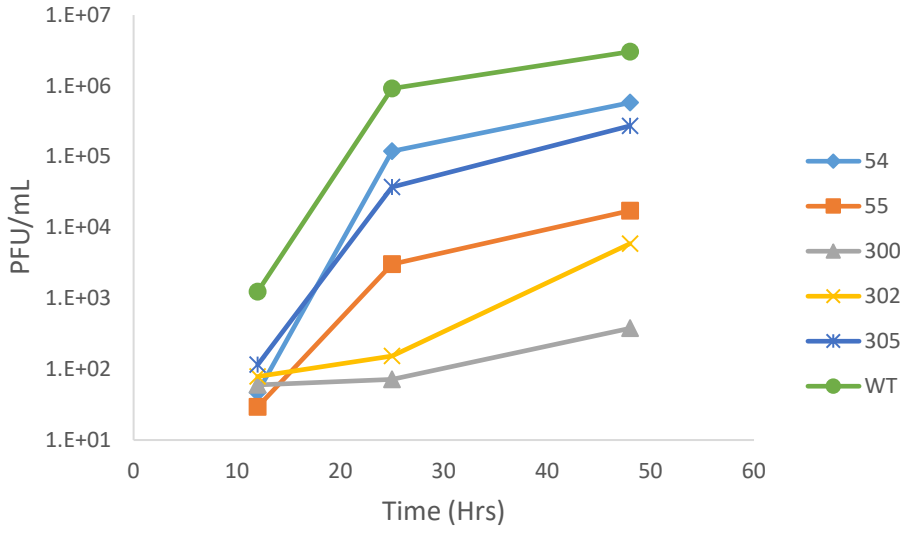

Figure 5. HPIV3 growth curve performed in HeLa cells. Cells were infected with virus at a MOI of 4 and virus samples were collected at 12, 24, and 48 hr time points, and titers were determined by plaque assay

Serial passages of the HPIV3 M mutant viruses were performed with the purpose of recovering a revertant virus at a second site to shed light on the reason for functional importance of these residues. Phenotypic revertants from viruses containing the Y300A and L305A amino acid substitutions were isolated. The L305A revertant contained a second-site mutation at the nucleotides encoding amino acid position 161 (glutamate to histidine, Hoffman lab unpublished). To confirm that the Q161H change is responsible for the reversion phenotype, a virus containing both changes (L305A/Q161H) was constructed, analyzed, and found to grow in a similar fashion to the isolated revertant (Fig. 6A).

The Y300A revertant had a mutation at the nucleotides encoding amino acid 289 resulting in an alanine to valine change. As with the L305A revertant, construction and analysis of a Y300A/A289V double mutant showed increased replicative ability (Fig. 6B). Neither of these reversions restored or created a late domain sequence providing further evidence the 300-YPLMDL region is not a late domain. In addition, the lack of a 3-D structure for HPIV3 M made hypotheses on the restoration of function these second site mutations caused difficult.

A

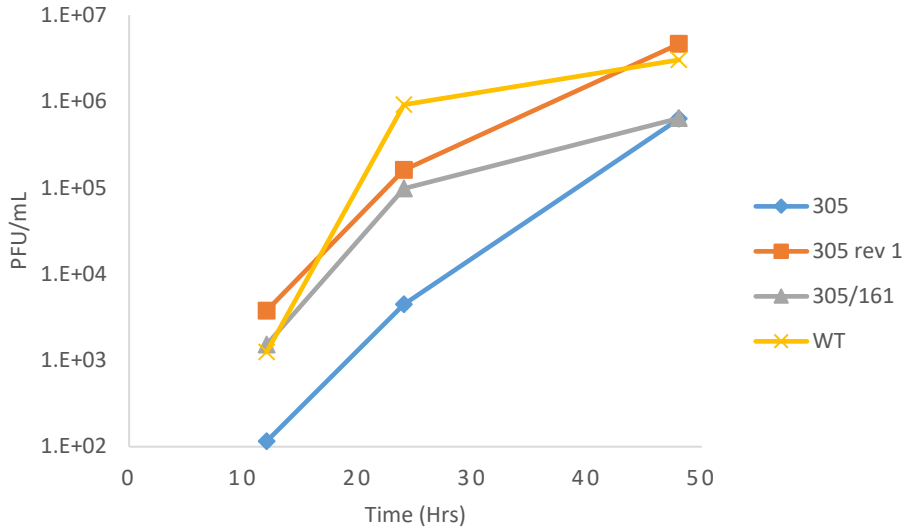

B

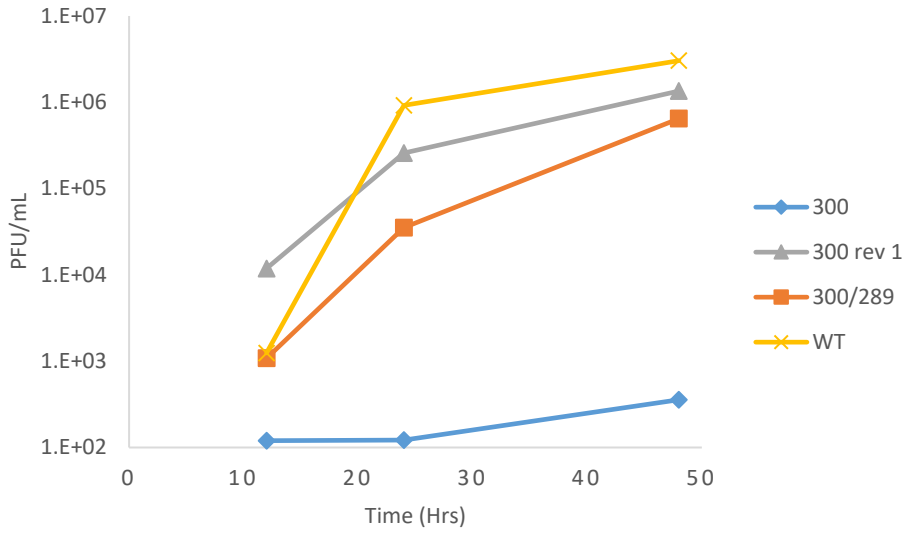

Figure 6. (A-B) HPIV3 growth curve performed in HeLa cells. Cells were infected with virus at a MOI of 4 and virus samples were collected at 12, 24, and 48 hr timepoints, and titers were determined by plaque assay

Research Objectives

To better understand the functions the 54-57 and 300-305 amino acid regions of

M the first research objective was to build a 3-D model of HPIV3-M. This model would

allow for predictions of the function of the 54, 55, 300, 302, and 305 residues. Completion of this research objective resulted in analysis of the original mutations and reversion mutations with structural models of HPIV3 M (based on the determined M protein crystal structure of the related NDV) (Fig. 7-9) (20). Analysis of the position of these amino acid residues resulted in the determination of M-M dimerization being the most likely importance of the 300, 302, and 305 residues (Fig. 7-9). Therefore my second objective was to determine if M-M interaction is affected in the alanine substitution mutants at the 300, 302, and 305 residues and if it is restored in the Y300A/A289V and L305A/Q161H mutants. My final objective was to assess if the localization of the previously mentioned M mutants is altered compared to WT-M

MATERIALS AND METHODS

Creation of a 3-D Homology Model

The structural model of HPIV3 M was generated by the SWISS-MODEL homology modelling program. HPIV3 M primary amino acid sequence was used as a target sequence (Uniprot id#:P0783). The resulting New Castle disease virus matrix protein (RCSB: 4G1G) was used as a template to build the model. The resulting model was viewed and imaged using Pymol (Schrodinger).

Cell Culture

Human embyonic kidney (HEK) 293T cells were cultured in Dulbecco's modified Eagle's medium (DMEM) with 10% fetal bovine serum and grown at 37°C with 5% CO2.

Plasmids

The pCAGGS Matrix (M) plasmid was previously constructed by inserting sequence encoding HPIV3 M into the pCAGGS vector. The Y300A, L302A, L305A, Y300A/A289V, and L305A/Q161H mutant M plasmids were generated via PCR site-directed mutagenesis of the pCAGGS-WT-M plasmid (26).

WT and mutant M sequences were inserted into the pACT and pBIND vector plasmids of the CheckMate™ Mammalian Two-Hybrid System (Promega corporation). *Sal*I and *Kpn*I sites were added to upstream and downstream primers to amplify the M open reading frame from the pCAGGS M plasmids via PCR. The subsequent PCR products and the pACT and pBIND vectors then underwent digestion

with *Sal*I and *Kpn*I enzymes and were gel purified. The PCR product containing the WT-M gene and mutant M genes were then ligated into the pACT and pBIND plasmids and transformed into *E. coli*. All plasmid sequences were confirmed by sequencing the insert region. Plasmids were purified using Qiagen© plasmid purification kits according to manufacturer's protocols.

Immunofluorescent Microscopy

Sub-confluent (40%) HEK-293T cells on glass coverslips were transfected with pCAGGS-M, or M mutants thereof. Transfections were performed in 6 well plates. The M plasmid, 0.5 μg, was added to 120 μl Opti-MEM™ (Gibco™ by Thermo Fisher Scientific) and 3 μl X-tremeGENE™ 9 DNA transfection reagent (Roche) at room temperature, allowed to sit for 30 min and then added to the cells. At varying time points post-transfection, cells were fixed with 4% formaldehyde for 10 min, permeabilized with 0.5% Triton X-100 (Sigma) in PBS twice for 2 min, and blocked with 8% milk in TBST for 30 min. The coverslips were incubated with a rabbit anti-M protein (1/100 dilution in TBST) for 1 hr, washed three times with TBST, and followed by a 1 hr incubation with a goat polyclonal anti-rabbit IgG antibody conjugated with Dylight 488 (1/200 dilution in TBST) (Abcam9683courtesy of Dr. Sanderfoot). Cells were washed twice with TBST, and incubated with 300 nM of DAPI (Thermo Fisher) in PBS for 5 min, then washed three times with PBS. The coverslips were then mounted on microscope slides with one drop of Fluoromount-G® (Southern Biotech) and sealed. A Nikon Eclipse 80i microscope and a Nikon CS1 Laser Scanning confocal fluorescence microscope were used for microscopic analysis, and images were analyzed with ImageJ (National Institutes of Health). To quantify the amount of M protein present in the nucleus the integrated

density in the nucleus and the integrated density of the total M protein present was determined. The integrated density of the M protein in the nucleus was divided by the integrated density of the M protein present throughout the whole cell to find the percent of the M protein present in the nucleus.

CheckMate™ Mammalian Two-Hybrid System

HEK-293T cells were seeded into 24-well plates and incubated for 18-24 hrs before transfection. pACT and pBIND plasmids, were combined in a molar ratio of 2:1, with the total amount of 0.135 µg DNA added. An equal amount (0.0675 µg) of pG5*luc v*ector was also added to each transfection reaction. Transfections were performed using Lipofectamine™ 3000 Transfection Reagent (Thermofisher Scientific). The luminescence activity was measured 24 hrs post transfection using the Dual-Luciferase® Reporter assay system (Promega corporation). Cells were lysed in 125 µl 1x passive lysis buffer. A single sample luminometer was used to measure light production. Either 1 µl or 5 µl of lysate was added to 25 µl of Luciferase Assay Reagent II and read for firefly luciferase activity. indicated an interaction of the fusion proteins Stop & Glo® Reagent (25 µl) was then added to quantitate Renilla luciferase activity as a normalization measure for transfection efficiency. pACT vector and pBIND vector without M inserts were used as a negative control. pACT vector and pBind with M insert was used as a background for WT-M and the M mutants. Binding efficiencies of mutants were calculated by comparing the increases in luciferase activity over background to the increase in luciferase activity over background of WT-M.

RESULTS

Generation of a 3-D Homology Model of HPIV3-M

In order to create predictions of the importance of amino acid regions of HPIV3-M a 3-D model homology model was created. The homology model was made with SWISS-model homology software using HPIV3-M as a target sequence and NDV-M protein as a template. The NDV M protein template used was recombinantly expressed and purified as a dimer (20). The NDV M protein structure was then determined using x-ray crystallography and deposited in the RCSB database with the identification number being, 4G1G (20). In the M dimer model, residues Y54 and L55 are found on a highly positive surface likely to interact with the plasma membrane, and so a disruption of the M-membrane interaction is possible (Fig. 7). It could also possibly be involved in a function before M reaches the membrane as well. The residues Y300, L302, and L305 are near the monomer surface between M dimers (Fig. 8). Additionally, the L305A/Q161H revertant provides evidence of the L305 residue being involved in M monomer-monomer interactions. Matrix protein residue Q161 is distant from L305 when observing the monomeric M protein. However, when observing position 305 on one monomer and position 161 on a neighboring monomer the two residues are in close proximity (Fig. 9). The recovery of this revertant, in addition to the presence of residue 305 at the monomeric surface, allows us to hypothesize that L305 may be important for M-M monomer to monomer interactions.

The explanation for the growth restoration by the A289V revertant of the Y300A mutant is not as clear. The amino acid position 289 is not near the dimer surface (Fig. 9). However since paramyxoviruses are known to form higher order oligomers, it is possible the change restored this ability of M (6). Additionally, the Y300 amino acid is still found near the monomeric surface, and so is likely important for dimerization.

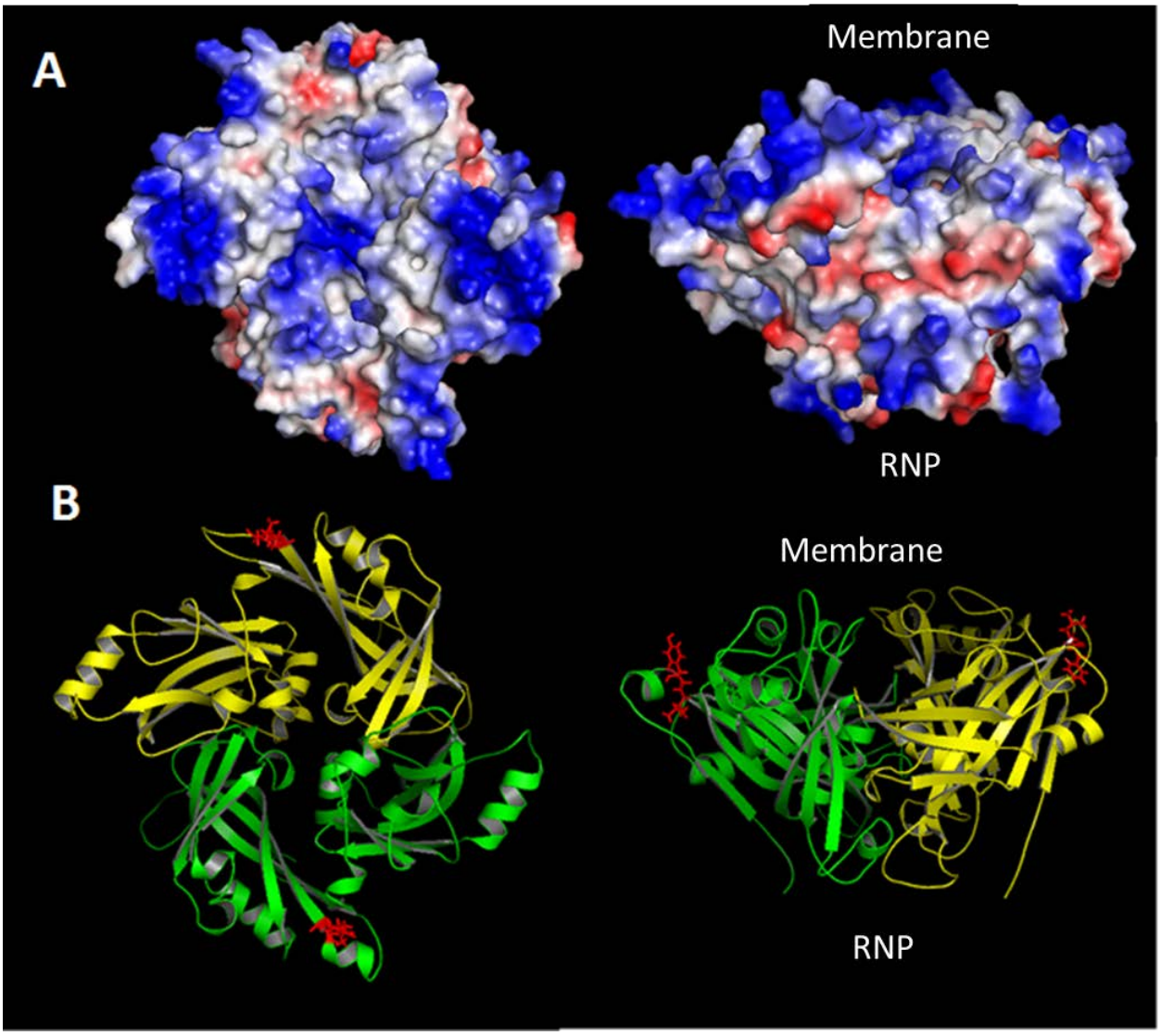

Figure 7. Human parainfluenza virus type 3 Matrix protein (HPIV3-M) model generated using SWISS-MODEL Homology Modelling (46-48). The right image is rotated 90^0 clockwise and 90^0 upward. (A) Surface model of HPIV3-M dimer with electrostatic potentials displayed in blue (positive) and red ((-)). (B) HPIV3-M monomers (green and yellow) in a ribbon diagram with residues 54 and 55 shown as red sticks.

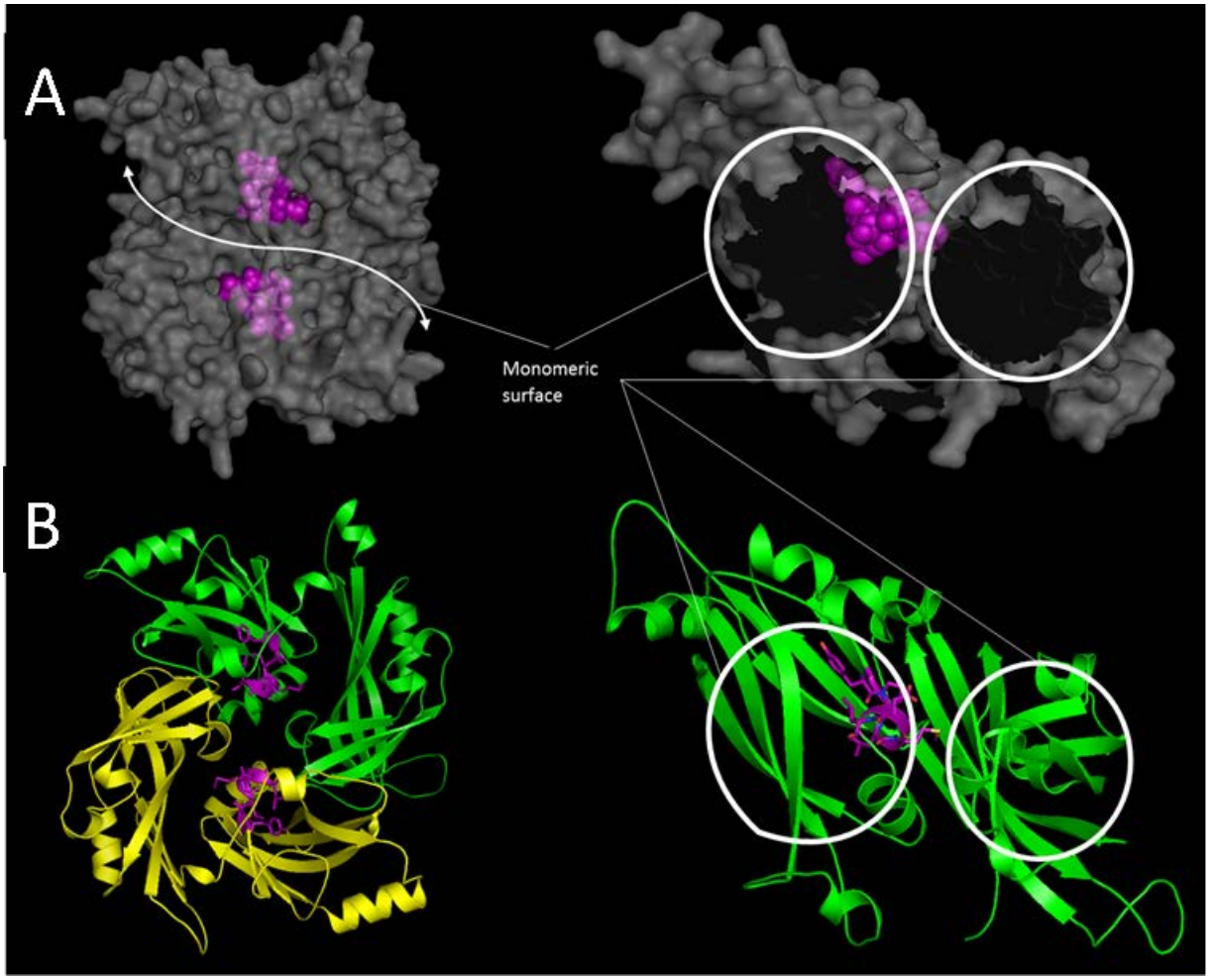

Figure 8. Human parainfluenza virus type 3 Matrix protein model generated using SWISS-MODEL homology modelling (45-47). Left images display M dimers and right images represent a 90^0 upward rotation of the L image with an M-monomer (yellow) hidden. (A) Surface representation in gray with aa300-305 shown as purple spheres. (B) Ribbon diagram with one monomer colored yellow and the other green, aa300-305 are colored purple with sticks shown.

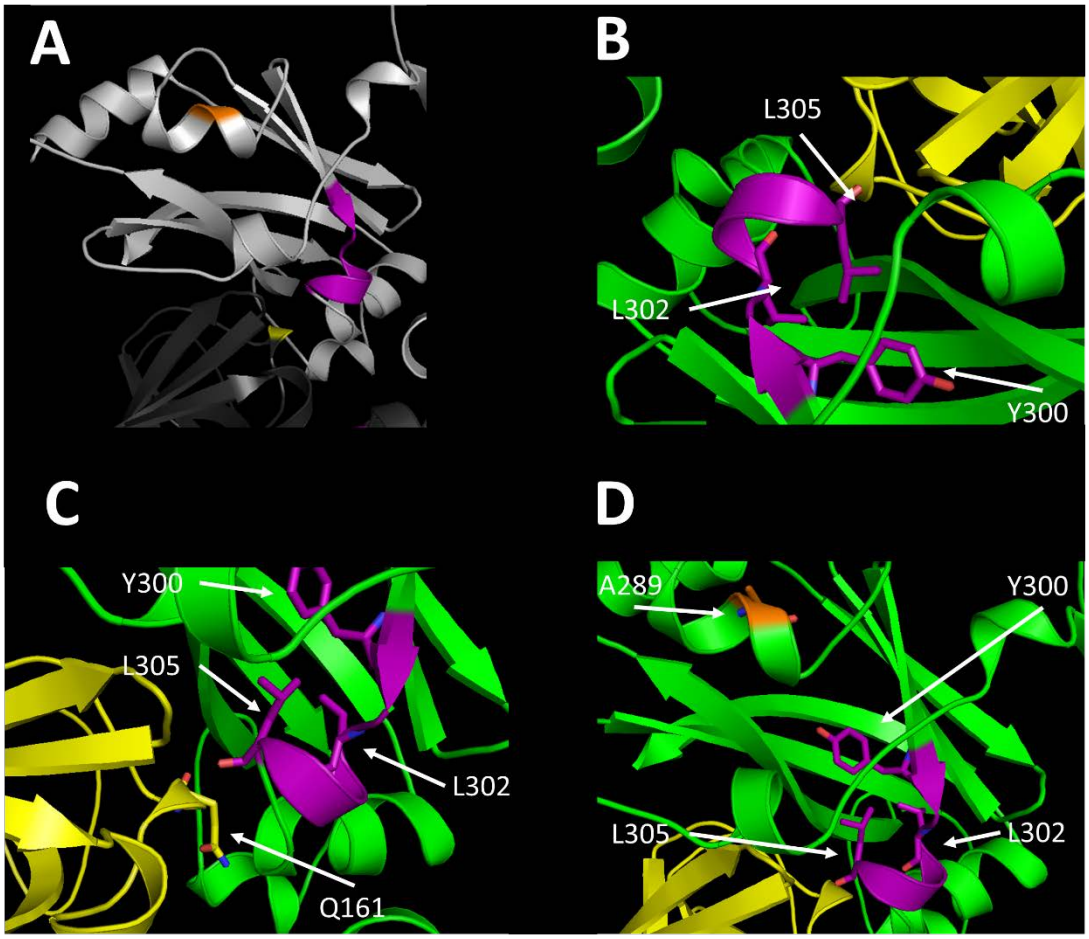

Figure 9. Sections of Human parainfluenza virus type 3 Matrix protein (dimer) model generated using SWISS-MODEL homology modelling (45-47). (A) (Monomer1=grey) (Monomer 2=black) Monomer 1 amino acids colored: aaA289-orange, aa300-YPLMDL-305-purple and monomer 2 amino acid Q161 colored yellow. (B-D) (Monomer1=Green) (Monomer 2=Yellow) Monomer 1 amino acids 300-YPLMDL-305 colored purple and aaY300, L302, and L305 shown as sticks. In (C) aaQ161 is yellow with sticks shown. In (D) aaA289 is orange with sticks shown.

Assessment of M Self-Association Disruption and Restoration.

Due to the location of the 300-305 amino acid residues being in proximity to the surface where monomeric M proteins interact to form a dimer, the M-M interaction (Fig 7-9) is likely an important function of these residues. To assess this hypothesis a mammalian 2-hybrid system (Checkmate, Promega) was utilized to investigate the self-interaction of M protein mutants (Y300A, L302A, L305A, Y300/A289A,

L305A/Q161H) and compare them to WT-M. Wild-type M and each mutant were inserted into the reading frames of the pACT and pBIND plasmids to create the M-activation domain and M-DNA binding domain fusions, respectively. Interaction of the resulting wild-type fusion M proteins resulted in transcription of a luciferase gene, which was measured by luciferase activity. The experiment was done in 5 replicates with duplicates performed in 4 of the replicates. The wild-type M-M interaction produced luciferase levels 2.7-fold over background levels (Table 1). Binding efficiencies of mutants were calculated by comparing the increases in luciferase activity over background to the increase in luciferase activity over background of WT-M. It was found that the single mutant M proteins (Y300A, L302A, L305A), which were defective in virus growth, were also significantly defective in M binding efficiencies compared to WT-M (Table 1). However, the growth restoration mutants (Y300/A289V, L305A/Q161H) M-M interactions were also defective compared to WT-M (Table 1). These results show amino acids 300, 302, and 305 are important for M-M dimerization. The results did not indicate a restoration of the M-M dimerization in the growth restoration mutants, and therefore the reason for growth restoration may not be restoration of M-M dimerization. Increasing higher order M-M interactions could still be possible since only dimerization is assessed using the mammalian two-hybrid system.

Table 1. Analysis of the self-association of 300-305 region mutants and revertants in the CheckMate™ Mammalian Two-Hybrid System

M insert Sequence	Mean fold increase	Mean M-M interaction compared to WT[a](%)
WT	2.7±0.2*	100
Y300A	1.2±0.1*	11±8
L302A	0.7±0.1	0±0
L305A	0.9±0.2	0±0.67
Y300A/A289V	1.1±0.2	6.54±10.24
L305A/Q161H	1.1±0.2	9.34±7.75

[a]M-M interaction assessed by increases in luciferase activity over expression of empty pACT vector and pBIND vector with the corresponding M insert.
*Statistically significant above background ($p<0.05$)

Assessment if localization is affected by perturbations of M.

Since localization of M proteins of the *Paramyxoviridae* have been shown to be important for the viral life cycle this function was investigated (22, 41-43). Two mutants (L302A and L305A) have also been investigated by another lab, Zhang et al., as a NES signal and ubiquitination control site (41). Therefore, I also used immunofluorescent microscopy to investigate the localization of various HPIV3 M proteins. The WT-M, Y300A-M, L302A-M, L305A-M, Y300A/A289V-M, and L305A/Q161H-M proteins were expressed individually in HEK-293T cells. At 24 hrs post-transfection the cells were fixed, and the nucleus and M proteins were stained for viewing via fluorescent microscopy. A minimum of 30 cells were viewed using both confocal and epifluorescent microscopy, and pixel intensities were measured to quantify the amount of M present in the nucleus and cytoplasm of cells. Nuclear localization of WT-M protein was found to be 31% ±9 (Table 2). The mutant M proteins (Y300A, L302A, L305A) and restoration mutant M proteins (Y300A/A289V, L305A/Q161H) did not have a statistical difference in nuclear localization compared to WT-M (Table 2). In addition to nuclear localization

the staining patterns of the various M mutants was similar to those seen in WT-M expressing cells (Fig. 10). These results show that alteration of amino acids Y300, L302, and L305 do not change the localization of the M protein.

Table 2. HPIV3 M protein nuclear localization.

M protein	Mean percentage nuclear (%)
WT	31±9
Y300A	34±8
L302A	31±10
L305A	29±10
Y300A/A289V	33±15
L305A/Q161H	32±11

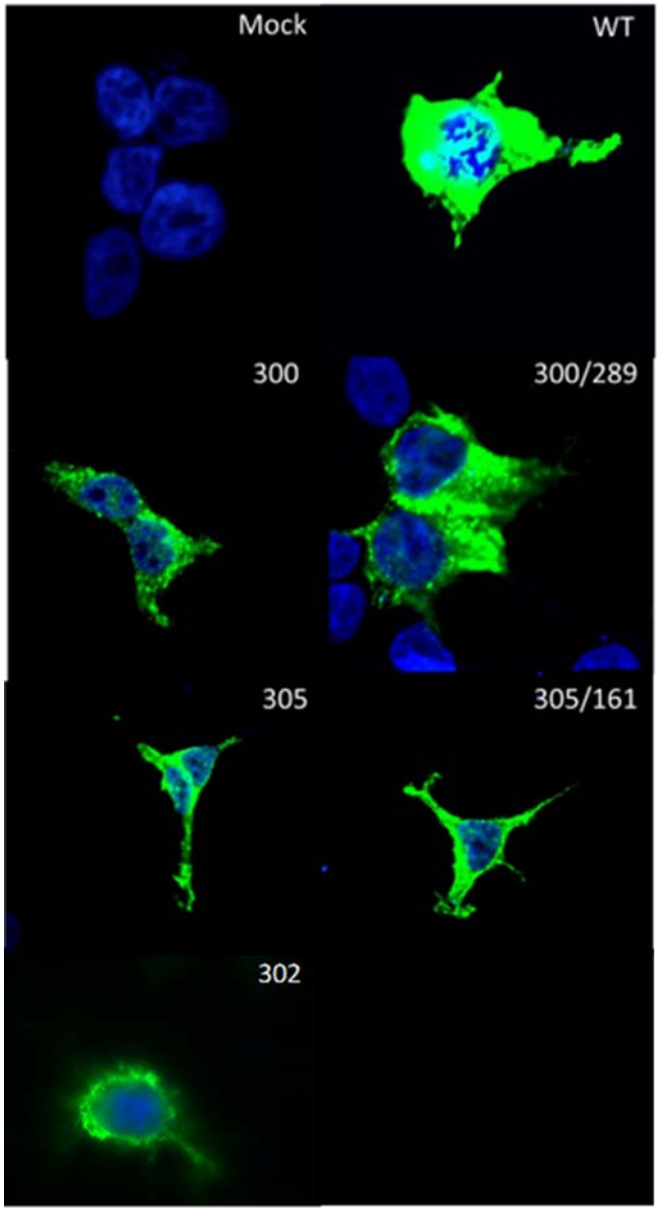

Figure 10. Localization of 300-305 region mutants and revertants thereof in 293T cells. 1 µg of WT-M, Y300A, Y300A/A289V, L305A, or L305A/Q161H encoding plasmids were transfected into 293T cells on coverslips. At 24 hr post-transfection, cells were fixed with 4% formaldehyde, permeabilized with 0.5% Triton X 100, and blocked with 5% milk TBST. Samples were then incubated with rabbit anti-M primary antibody followed by an anti-rabbit secondary antibody conjugated with Dylight 488. Cells were stained with DAPI to visualize the nuclei. Samples were imaged at 600x with confocal microscopy

DISCUSSION

Matrix proteins of paramyxoviruses have been shown to be essential in assembly and release of virions through their multiple interactions. Through alanine substitution mutagenesis the 300-305 amino acid sequences of HPIV3 M have been identified by the Hoffman lab as being important for generation of VLPs and growth of virus (Fig 3-6). Additionally, serially passaging of mutant M viruses (Y300A, L305A) resulted in isolation of two revertants containing second-site mutations in the M protein (Y300A/A289V, L305A/Q161H). In viewing the position of the original M mutants and possible reversion mutations in the 3-D model, it is likely these residues are important for M-M self-association (Fig 7-9).

Self-association of M has been shown in related viruses such as canine distemper virus and respiratory syncytial virus to be important for localization of M and membrane budding activity (24, 74). Given this evidence I investigated whether the HPIV3 M mutants in the 300-305 region lost M self-association using a mammalian 2-hybrid system. Additionally, I investigated whether the growth restoration mutant M proteins (Y300A/A289V, L305A/Q161H) restored M self-association. Two of the mutants investigated (L302A and L305A) have also been investigated by another lab, Zhang et al., and L302A was proposed to be part of a NES signal and control ubiquitination (41). Therefore, I also used immunofluorescent microscopy to investigate the localization of the following M mutants: Y300A, L302A, L305A, Y300A/A289V, L305A/Q161H.

The mammalian 2-hybrid results supported the prediction based on the 3-D model of HPIV3 M, that the 300-305 amino acid sequence is involved in M-M self-association. The system used showed a 2.7-fold increase in luciferase activity over background for WT-M self-association. Although the WT-M signal was only 2.7-fold higher, it was shown to be consistently above background. In contrast, the L302A and L305A mutant M proteins never produced a signal over background. The Y300A M mutant only produced an 11% increase in signal compared with WT-M (Table 1). This was a statistically significant increase in signal above background, but was still significantly below WT-M (Table 1). These results show that mutations in this region affect the binding efficiency of HPIV3 M proteins. However, the system did not show the growth restoration M mutants (Y300A/A289V, L305/Q161H) to have restored M-M binding ability. The Y300A/A289V M had a slight increase over background, but it was similar to the levels seen in the Y300A mutant. The L305A/Q161H M also had a slight insignificant increase in signal over the L305A mutant and background. Given that the WT-M was only 2.7 fold over background it's entirely possible this assay does not have the resolving power to distinguish a slight increase over background with the two restoration mutants. Alternative approaches may help determine whether the growth restoration mutants have increase M-M association, this could be done by attempting to co-immunoprecipitate the growth restoration mutants with WT-M. Alternatively, the growth restoration phenotype could also be due to some other function of the M protein such as: membrane binding or interactions with other viral proteins. The fact is, we do not know what impact decreased M-M association has on other activities of the M protein.

In addition to investigating the self-association of M, I also studied the localization of aa300-305 alanine substitution mutants and revertants using immunofluorescence microscopy. M mutants deficient in growth (Y300A, L302A, L305A) did not have a significant difference in nuclear localization compared to WT-M (Table 2). Additionally, reversion mutant M proteins (Y300A/A289V, L305A/Q161H) had similar nuclear localization as WT-M. Since mutation of these residues did not affect localization, it is unlikely nuclear trafficking is the function of this region. This finding also indicates that regions of the mutant M proteins structure are likely maintained despite the mutations, since they are still able to traffic through the cell in a similar manner to WT-M proteins.

As mentioned earlier, two of the mutant HPIV3 M proteins have also been investigated by the Zhang et al. lab. Zhang claims, through immunofluorescence microscopy that the L302A M mutant was unable to target the plasma membrane (41). The authors did not offer any quantitative analysis of either nuclear localization or plasma membrane localization using their immunofluorescence data. They did show, via a membrane association assay, that L302A had less membrane association than WT-M. I did not find the nuclear localization or plasma membrane localization of the L302A M mutant to be any different from WT-M when viewing them using immunofluorescence microscopy. The conflicting results could be due to Zhang et. al. using a tagged version of the M protein. A membrane association assay using untagged L302A M could possibly resolve this discrepancy.

Also, in contrast to my results, Zhang et.al. showed L302A M to retain interactions with WT-M protein through coimmunoprecipitations (41). A possible

explanation for the differing results is that I studied interactions between mutant proteins with itself and not with tagged, WT-M proteins. Studying the self-association (rather than mutant-WT association) of the mutants and revertants better reflects the physiological conditions, since WT-M would not be present in the various mutant and revertant viruses studied. Another possible explanation for the discrepant results is the fact that protein binding with the mammalian 2-hybrid system occurs in the nucleus of the cells while the coimmunoprecipitation looks at cytosolic interactions of proteins.

Overall I've shown the 300-305 region is important for self-association of the HPIV3 M protein. This loss of self-association inhibits the ability of HPIV3 to replicate ~~itself~~ because mutating this region affects growth curves of HPIV3. However, the loss of self-association of the HPIV3 M mutants does not seem to affect localization of the protein. The negative effects of the 300 and 305 mutations on virus replication are restored in revertants of the Y300A and L305A mutants. It is still not clear whether the reversion mutations restore the loss of self-association or affect another function of the HPIV3 M protein remains to be determined. Generation of mutant viruses containing only the second site amino acid change in M could be done to confirm the second site change growth restoration is related to the first change. Additionally, cross-linking studies of the various M proteins analyzed could be done to further investigate whether dimerization and/or oligomerization is affected by the various amino acid changes. Finally, assessing if interactions with other viral proteins remain intact with the M proteins tested would help determine if the M-M dimerization is the only function affected by the amino acid changes.

REFERENCES

1. Henrickson K. 2003. Parainfluenza Viruses. Clin Microbiol Rev 16:242-264. https://jvi.asm.org/sites/default/files/additional-assets/JVI-ITA.pdf
2. Jamison D. 2006. Disease control priorities in developing countries, 2nd ed. Oxford University Press, New York.

3. Rudan I. 2008. Epidemiology and etiology of childhood pneumonia. Bull World Health Org 86:408-416.

4. O'Brien K, Baggett H, Brooks W, Feikin D, Hammitt L, Higdon M, Howie S, Deloria Knoll M, Kotloff K, Levine O, Madhi S, Murdoch D, Prosperi C, Scott J, Shi Q, Thea D, Wu Z, Zeger S, Adrian P, Akarasewi P, Anderson T, Antonio M, Awori J, Baillie V, Bunthi C, Chipeta J, Chisti M, Crawley J, DeLuca A, Driscoll A, Ebruke B, Endtz H, Fancourt N, Fu W, Goswami D, Groome M, Haddix M, Hossain L, Jahan Y, Kagucia E, Kamau A, Karron R, Kazungu S, Kourouma N, Kuwanda L, Kwenda G, Li M, Machuka E, Mackenzie G, Mahomed N, Maloney S, McLellan J, Mitchell J, Moore D, Morpeth S, Mudau A, Mwananyanda L, Mwansa J, Silaba Ominde M, Onwuchekwa U, Park D, Rhodes J, Sawatwong P, Seidenberg P, Shamsul A, Simões E, Sissoko S, Wa Somwe S, Sow S, Sylla M, Tamboura B, Tapia M, Thamthitiwat S, Toure A, Watson N, Zaman K, Zaman S. 2019. Causes of severe pneumonia requiring hospital admission in children without HIV infection from Africa and Asia: the PERCH multi-country case-control study. The Lancet 394:757-779.

5. Glezen W, Frank A, Taber L, Kasel J. 1984. Parainfluenza Virus Type 3: Seasonality and Risk of Infection and Reinfection in Young Children. J Infect Dis 150:851-857.

6. Zuckerman A. 2009. Principles and practice of clinical virology. John Wiley & Sons, Chichester, West Sussex.

7. King A. 2012. Virus taxonomy. Elsevier, London.

8. Fields B, Knipe D, Howley P. 2013. Fields virology. Wolters Kluwer Health/Lippincott Williams & Wilkins, Philadelphia.

9. Maclachlan N, N. James Maclachlan E, Winton J. 2016. Fenner's Veterinary Virology (Fifth Edition). Academic Press, [S.l.].

10. Qureshi Adnan I. Ebola virus disease.

11. Knust B, Schafer I, Wamala J, Nyakarahuka L, Okot C, Shoemaker T, Dodd K, Gibbons A, Balinandi S, Tumusiime A, Campbell S, Newman E, Lasry E, DeClerck H, Boum Y, Makumbi I, Bosa H, Mbonye A, Aceng J, Nichol S, Ströher U, Rollin P. 2015. Multidistrict Outbreak of Marburg Virus Disease—Uganda, 2012. J Infect Dis 212:S119-S128.

12. Mahy B, Van Regenmortel M. 2008. Encyclopedia of virology. Elsevier, [New York].

13. Kingsbury D. 1991. The Paramyxoviruses. Plenum Press, New York.

14. Malur A, Hoffman M, Banerjee A. 2004. The human parainfluenza virus type 3 (HPIV 3) C protein inhibits viral transcription. Virus Research 99:199-204.

15. Shil N, Pokharel S, Banerjee A, Hoffman M, Bose S. 2017. Inflammasome antagonism by human parainfluenza virus type 3 C protein. J Virol 92:e01776-17.

16. Yin H, Paterson R, Wen X, Lamb R, Jardetzky T. 2005. Structure of the uncleaved ectodomain of the paramyxovirus (hPIV3) fusion protein. Proceedings of the National Academy of Sciences 102:9288-9293.

17. Waning D, Schmitt A, Leser G, Lamb R. 2002. Roles for the Cytoplasmic Tails of the Fusion and Hemagglutinin-Neuraminidase Proteins in Budding of the Paramyxovirus Simian Virus 5. J Virol 76:9284-9297.

18. Lyles D. 2013. Assembly and Budding of Negative-Strand RNA Viruses. Adv Virus Res 85:57-90.

19. Harrison M, Sakaguchi T, Schmitt A. 2010. Paramyxovirus assembly and budding: Building particles that transmit infections. Int J Biochem Cell Biol 42:1416-1429.

20. Battisti A, Meng G, Winkler D, McGinnes L, Plevka P, Steven A, Morrison T, Rossmann M. 2012. Structure and assembly of a paramyxovirus matrix protein. Proc Natl Acad Sci 109:13996-14000.

21. Waning D, Schmitt A, Leser G, Lamb R. 2002. Roles for the Cytoplasmic Tails of the Fusion and Hemagglutinin-Neuraminidase Proteins in Budding of the Paramyxovirus Simian Virus 5. J Virol 76:9284-9297.

22. Pantua H, McGinnes L, Peeples M, Morrison T. 2006. Requirements for the Assembly and Release of Newcastle Disease Virus-Like Particles. J Virol 80:11062-11073.

23. Pentecost M, Vashisht A, Lester T, Voros T, Beaty S, Park A, Wang Y, Yun T, Freiberg A, Wohlschlegel J, Lee B. 2015. Evidence for Ubiquitin-Regulated Nuclear and

Subnuclear Trafficking among *Paramyxovirinae* Matrix Proteins. PLOS Pathog 11:e1004739.

24. Förster A, Maertens G, Farrell P, Bajorek M. 2015. Dimerization of Matrix Protein Is Required for Budding of Respiratory Syncytial Virus. J Virol 89:4624-4635.

25. Irie T, Shimazu Y, Yoshida T, Sakaguchi T. 2006. The YLDL Sequence within Sendai Virus M Protein Is Critical for Budding of Virus-Like Particles and Interacts with Alix/AIP1 Independently of C Protein. J Virol 81:2263-2273.

26. Bracken M, Hoffman M, Kandel S, Hayes B, Ackerson L, Scott-Shemon D. 2016. Viral protein requirements for assembly and release of human parainfluenza virus type 3 virus-like particles. J Virol 97:1305-1310.

27. Schmitt A, Leser G, Waning D, Lamb R. 2002. Requirements for Budding of Paramyxovirus Simian Virus 5 Virus-Like Particles. J Virol 76:3952-3964.

28. Li M, Schmitt P, Li Z, McCrory T, He B, Schmitt A. 2009. Mumps Virus Matrix, Fusion, and Nucleocapsid Proteins Cooperate for Efficient Production of Virus-Like Particles. J Virol 83:7261-7272.

29. Wirblich C, Tan G, Papaneri A, Godlewski P, Orenstein J, Harty R, Schnell M. 2008. PPEY Motif within the Rabies Virus (RV) Matrix Protein Is Essential for Efficient Virion Release and RV Pathogenicity. J Virol 82:9730-9738.

30. Craven RC, Harty RN, Paragas J, Palese P, Wills JW. Late domain function identified in the vesicular stomatitis virus M protein by use of rhabdovirus-retrovirus chimeras. J Virol. 1999;73:3359–65.

31. Harty RN, Paragas J, Sudol M, Palese P. A proline-rich motif within the matrix protein of vesicular stomatitis virus and rabies virus interacts with WW domains of cellular proteins: implications for viral budding. J Virol. 1999;73:2921–9.

32. Jayakar HR, Murti KG, Whitt MA. Mutations in the PPPY motif of vesicular stomatitis virus matrix protein reduce virus budding by inhibiting a late step in virion release. J Virol. 2000;74:9818–27.

33. Harty RN, Brown ME, Wang G, Huibregtse J, Hayes FP. A PPxY motif within the VP40 protein of Ebola virus interacts physically and functionally with a ubiquitin ligase: implications for filovirus budding. Proc Natl Acad Sci USA. 2000;97:13871–6.

34. Licata JM, Simpson-Holley M, Wright NT, Han Z, Paragas J, Harty RN. Overlapping motifs (PTAP and PPEY) within the Ebola virus VP40 protein function independently as late budding domains: involvement of host proteins TSG101 and VPS-4. J Virol. 2003;77:1812–9.

35. Martin-Serrano J, Zang T, Bieniasz PD. HIV-1 and Ebola virus encode small peptide motifs that recruit Tsg101 to sites of particle assembly to facilitate egress. Nat Med. 2001;7:1313–9.

36. Perez M, Craven RC, de la Torre JC. The small RING finger protein Z drives arenavirus budding: implications for antiviral strategies. Proc Natl Acad Sci USA. 2003;100:12978–83.

37. Utley TJ, Ducharme NA, Varthakavi V, Shepherd BE, Santangelo PJ, Lindquist ME, et al. Respiratory syncytial virus uses a Vps4-independent budding mechanism controlled by Rab11-FIP2. Proc Natl Acad Sci USA. 2008;105:10209–14.

38. Patch JR, Han Z, McCarthy SE, Yan L, Wang LF, Harty RN, et al. The YPLGVG sequence of the Nipah virus matrix protein is required for budding. Virol J. 2008;5:1.
39. Henne W, Buchkovich N, Emr S. 2011. The ESCRT Pathway. Developmental Cell 21:77-91.

40. Bieniasz PD. Late budding domains and host proteins in enveloped virus release. Virology. 2006;344:55–63.

41. Zhang G, Zhang S, Ding B, Yang X, Chen L, Yan Q, Jiang Y, Zhong Y, Chen M. 2014. A Leucine Residue in the C Terminus of Human Parainfluenza Virus Type 3 Matrix Protein Is Essential for Efficient Virus-Like Particle and Virion Release. J Virol 88:13173-13188.

42. Coleman N, Peeples M. 1993. The Matrix Protein of Newcastle Disease Virus Localizes to the Nucleus via a Bipartite Nuclear Localization Signal. Virology 195:596-607.

43. Ghildyal R, Ho A, Wagstaff K, Dias M, Barton C, Jans P, Bardin P, Jans D. 2005. Nuclear Import of the Respiratory Syncytial Virus Matrix Protein Is Mediated By Importin β1 Independent of Importin α†. Biochemistry 44:12887-12895.

44. Wang Y, Park A, Lake M, Pentecost M, Torres B, Yun T, Wolf M, Holbrook M, Freiberg A, Lee B. 2010. Ubiquitin-Regulated Nuclear-Cytoplasmic Trafficking of the Nipah Virus Matrix Protein Is Important for Viral Budding. PLoS Path 6:e1001186.

45. Harrison M, Schmitt P, Pei Z, Schmitt A. 2012. Role of Ubiquitin in Parainfluenza Virus 5 Particle Formation. J Virol 86:3474-3485.

46. Marco Biasini; Stefan Bienert; Andrew Waterhouse; Konstantin Arnold; Gabriel Studer; Tobias Schmidt; Florian Kiefer; Tiziano Gallo Cassarino; Martino Bertoni; Lorenza Bordoli; Torsten Schwede. (2014). SWISS-MODEL: modelling protein tertiary and quaternary structure using evolutionary information. Nucleic Acids Research (1 July 2014) 42 (W1): W252-W258; doi: 10.1093/nar/gku340.

47. Arnold, K., Bordoli, L., Kopp, J. and Schwede, T. (2006) The SWISS-MODEL workspace: a web-based environment for protein structure homology modelling. Bioinformatics, 22, 195-201.

48. Benkert, P., Biasini, M. and Schwede, T. (2011) Toward the estimation of the absolute quality of individual protein structure models. Bioinformatics, 27, 343-350.

49. 2016. UniProt: the universal protein knowledgebase. Nucleic Acids Research 45:D158-D169.

50. Cattaneo R, Schmid A, Rebmann G, Baczko K, Ter Meulen V, Bellini W, Rozenblatt S, Billeter M. 1986. Accumulated measles virus mutations in a case of subacute sclerosing panencephalitis: Interrupted matrix protein reading frame and transcription alteration. Virology 154:97-107.

51. Cathomen T, Mrkic B, Spehner D, Drillien R, Naef R, Pavlovic J, Aguzzi A, Billeter M, Cattaneo R. 1998. A matrix-less measles virus is infectious and elicits extensive cell fusion: consequences for propagation in the brain. The EMBO Journal 17:3899-3908.

52. Inoue M, Tokusumi Y, Ban H, Kanaya T, Shirakura M, Tokusumi T, Hirata T, Nagai Y, Iida A, Hasegawa M. 2003. A New Sendai Virus Vector Deficient in the Matrix Gene Does Not Form Virus Particles and Shows Extensive Cell-to-Cell Spreading. J Virol 77:6419-6429.

53. Coronel EC, Murti KG, Takimoto T, Portner A. Human parainfluenza virus type 1 matrix and nucleoprotein genes transiently expressed in mammalian cells induce the release of virus- like particles containing nucleocapsid-like structures. J Virol. 1999;73:7035–8.

54. Sugahara F, Uchiyama T, Watanabe H, Shimazu Y, Kuwayama M, Fujii Y, et al. Paramyxovirus Sendai virus-like particle formation by expression of multiple viral proteins and acceleration of its release by C protein. Virology. 2004;325:1–10.

55. Takimoto T, Murti KG, Bousse T, Scroggs RA, Portner A. Role of matrix and fusion proteins in budding of sendai virus. J Virol. 2001;75:11384–91.

56. Ciancanelli MJ, Basler CF. Mutation of YMYL in the Nipah virus matrix protein abrogates budding and alters subcellular localization. J Virol. 2006;80:12070–8.

57. Pohl C, Duprex WP, Krohne G, Rima BK, Schneider-Schaulies S. Measles virus M and F proteins associate with detergent-resistant membrane fractions and promote formation of virus-like particles. J Gen Virol. 2007;88:1243–50.

58. Runkler N, Pohl C, Schneider-Schaulies S, Klenk H-D, Maisner A. Measles virus nucleocapsid transport to the plasma membrane requires stable expression and surface accumulation of the viral matrix protein. Cell Microbiol. 2007;9:1203–14.

59. Ghildyal R, Ho A, Dias M, Soegiyono L, Bardin PG, et al. (2009) The respiratory syncytial virus matrix protein possesses a Crm1-mediated nuclear export mechanism. J Virol 83: 5353–5362.

60. Duan Z, Song Q, Wang Y, He L, Chen J, et al. (2013) Characterization of signal sequences determining the nuclear export of Newcastle disease virus matrix protein. Arch Virol 158: 2589–2595.

61. Duan Z, Li Q, He L, Zhao G, Chen J, et al. (2013) Application of green fluorescent protein-labeled assay for the study of subcellular localization of Newcastle disease virus matrix protein. J Virol Methods 194: 118–122.

62. Yoshida T, Nagai Y'Yoshii S, Maeno K, Matsumoto T (1976) Membrane (M) protein of HVJ (Sendai virus): its role in virus assembly. Virology 71: 143–161.

63. Bjellqvist, B.,Hughes, G.J., Pasquali, Ch., Paquet, N., Ravier, F., Sanchez, J.-Ch., Frutiger, S. & Hochstrasser, D.F. The focusing positions of polypeptides in immobilized pH gradients can be predicted from their amino acid sequences. Electrophoresis 1993, 14, 1023-1031.

64. Bjellqvist, B., Basse, B., Olsen, E. and Celis, J.E. Reference points for comparisons of two-dimensional maps of proteins from different human cell types defined in a pH scale where isoelectric points correlate with polypeptide compositions. Electrophoresis 1994, 15, 529-539.

65. Gasteiger E., Hoogland C., Gattiker A., Duvaud S., Wilkins M.R., Appel R.D., Bairoch A.;Protein Identification and Analysis Tools on the ExPASy Server; (In) John M. Walker (ed): The Proteomics Protocols Handbook, Humana Press (2005).

66. Ali A, Nayak DP. Assembly of Sendai virus: M protein interacts with F and HN proteins and with the cytoplasmic tail and transmembrane domain of F protein. Virology. 2000;276:289–303.

67. Henderson G. Sorting of the Respiratory Syncytial Virus Matrix Protein into Detergent-Resistant Structures Is Dependent on Cell-Surface Expression of the Glycoproteins. Virology. 2002;300:244–54.

68. Iwasaki M, Takeda M, Shirogane Y, Nakatsu T, Nakamura T, Yanagi Y. The matrix protein of measles virus regulates viral RNA synthesis and assembly by interacting with the nucleocapsid protein. J Virol. 2009;83:10374–83.

69. 5. Markwell M, Fox C. 1980. Protein-Protein Interactions Within Paramyxoviruses Identified by Native Disulfide Bonding or Reversible Chemical Cross-Linking. J Virol 33:152-166.

70. Nagai Y, Yoshida T, Hamaguchi M, Iinuma M, Maeno K, Matsumoto T. 1978. Cross-linking of Newcastle disease virus (NDV) proteins. Arch Virol 58:15-28.

71. Sagrera A, Cobaleda C, Berger S, Marcos M, Shnyrov V, Villar E. 1998. Study of the influence of salt concentration on Newcastle disease virus matrix protein aggregation. IUBMB Life 46:429-435.

72. Ravid D, Leser G, Lamb R. 2010. A Role for Caveolin 1 in Assembly and Budding of the Paramyxovirus Parainfluenza Virus 5. J Virol 84:9749-9759.

73. Koga R, Kubota M, Hashiguchi T, Yanagi Y, Ohno S. 2018. Annexin A2 Mediates the Localization of Measles Virus Matrix Protein at the Plasma Membrane. J Virol 92:e00181-18.

74. Bringolf F, Herren M, Wyss M, Vidondo B, Langedijk J, Zurbriggen A, Plattet P. 2017. Dimerization Efficiency of Canine Distemper Virus Matrix Protein Regulates Membrane-Budding Activity. J Virol 91:e00521-17.

75. Liu Y, Grusovin J, Adams T. 2018. Electrostatic interactions between Hendra virus matrix proteins are required for efficient virus-like particle assembly. J Virol JVI.00143-18.

76. Hulseberg C. 2011. Master's thesis. University of Wisconsin-La Crosse, La Crosse, WI. Identification of a novel late domain in human parainfluenza virus type 3 matrix protein.

77. Money V, McPhee H, Mosely J, Sanderson J, Yeo R. 2009. Surface features of a Mononegavirales matrix protein indicate sites of membrane interaction. Proceedings of the National Academy of Sciences 106:4441-4446.

78. Suresh K. 2016. Master's thesis. University of Wisconsin-La Crosse, La Crosse, WI. The cellular protein Alix does not have an apparent role in human parainfluenza virus type 3 budding.

79. Gosselin-Grenet A, Marq J, Abrami L, Garcin D, Roux L. 2007. Sendai virus budding in the course of an infection does not require Alix and VPS4A host factors. Virology 365:101-112.